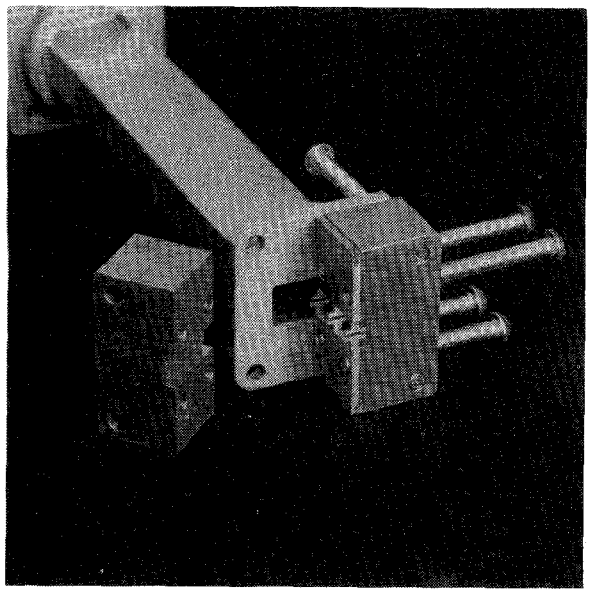

Fig. 4. Photograph of the opened evanescent-mode T-septum waveguide filter prototype with feeding X-band waveguide.

be responsible for the measured noise at beyond-X-band frequencies. Except for these limitations, however, close agreement between theoretical and experimental data is obtained over the entire measured frequency range. This indicates that a fabrication procedure utilizing modern production facilities will cause the evanescent-mode filter to respond as predicted.

Fig. 4 shows a photograph of the opened evanescent-mode T-septum waveguide filter prototype with the feeding X-band waveguide. A split-block waveguide housing is used to sandwich the two T-septum inserts. Note that due to the high bandwidth of the T-septum waveguide, i.e., its capability to significantly reduce the cutoff frequency compared to a ridge waveguide of identical housing dimensions, the filter component is extremely small. With an overall length of less than 3/4 inches, this design is one of the most space-efficient bandpass configurations proposed so far in waveguide technology.

IV. Conclusions

The theoretical treatment of the T-septum waveguide by mode-matching techniques forms a powerful tool for the computer-aided design of evanescent-mode filter applications. Through the incorporation of higher-order mode interactions, the proposed model provides design data which are in close agreement with experiments as is demonstrated at the example of an X-band filter prototype. The broadband characteristics of the T-septum waveguide make it possible, first, to improve the stopband behavior compared to common evanescent-mode configurations and, secondly, to reduce the filter size considerably. The length of the three-resonator prototype measures approximately one third of the guide wavelength at midband frequency.

References

[1] G. Craven and C. K. Mok, "The design of evanescent mode waveguide band-pass filters for a prescribed insertion loss characteristic," *IEEE Trans. Microwave Theory Tech.*, vol. MTT-19, pp. 295–308, Mar. 1971.

[2] H. F. Chappell, "Waveguide low pass filter using evanescent mode inductors," *Microwave J.*, vol. 21, pp. 71–72, Dec. 1978.

[3] R. Vahldieck and W. J. R. Hoefer, "Computer-aided design of dielectric resonator filters in waveguide sections below cutoff," *Electron. Lett.*, vol. 21, pp. 843–844, Sept. 1985.

[4] J.-W. Tao and H. Baudrand, "Multimodal variational analysis of uniaxial waveguide discontinuities," *IEEE Trans. Microwave Theory Tech.*, vol. 39, pp. 506–516, Mar. 1991.

[5] Q. Zhang and T. Itoh, "Computer-aided design of evanescent-mode waveguide filters with non-touching E-plane fins," *IEEE Trans. Microwave Theory Tech.*, vol. 36, pp. 404–412, Feb. 1988.

[6] Y. Zhang and W. T. Joines, "Some properties of T-septum waveguides," *IEEE Trans. Microwave Theory Tech.*, vol. MTT-35, pp. 769–775, Aug. 1987.

[7] V. A. Labay and J. Bornemann, "Singular value decomposition improves accuracy and reliability of T-septum waveguide field-matching analysis," *Int. J. MIMICAE*, vol. 2, pp. 82–89, Apr. 1992.

[8] J. Bornemann and F. Arndt, "Transverse resonance, standing wave, and resonator formulations of the ridge waveguide eigenvalue problem and its application to E-plane finned waveguide filters," *IEEE Trans. Microwave Theory Tech.*, vol. 38, pp. 1104–1113, Aug. 1990.

[9] Y. C. Shih, "The mode-matching method," in *Numerical Techniques For Microwave And Millimeter-Wave Passive Structures*, T. Itoh, Ed., New York: Wiley, 1989, ch. 9.

[10] L. Q. Bui, D. Ball and T. Itoh, "Broad-band millimeter-wave E-plane bandpass filters," *IEEE Trans. Microwave Theory Tech.*, vol. MTT-32, pp. 1655–1658, Dec. 1984.

[11] J. W. Bandler and S. H. Chen, "Circuit optimization: The state of the art," *IEEE Trans. Microwave Theory Tech.*, vol. 36, pp. 424–443, Feb. 1988.

Asymptotic Analysis of Mode Transition in General Class of Circular Hollow Waveguides at the Infrared Frequency

Yuji Kato and Mitsunobu Miyagi

***Abstract*—Correspondence between hybrid modes in small and large core circular hollow waveguides is discussed by using an asymptotic theory for the infrared. The mode changes or mode transitions in several hollow waveguides are discussed which depend on the cladding material and the mode order. For the dielectric-coated metallic waveguides, mode changes also depend on the thickness of the coated dielectric. For the singly cladded hollow waveguides, the region is shown in the plane of complex refractive index $(n - jk)$ of cladding material where the HE_{11} mode in large core waveguides approaches the TE or TM mode.**

I. Introduction

Hollow waveguides are important media in the wavelengths where bulky losses of materials are too high to achieve low-loss flexible fibers and also media for high-powered laser light transmission where the reflections at input and output ends of waveguides can be neglected [1]. Therefore, the waveguides have been recently regarded a candidate for high-powered CO_2 laser light [2] and infrared radiometry [3].

Mode properties of circular hollow waveguides were already discussed in detail [1] when the core diameter is large. Due to needs

Manuscript received February 28, 1992; revised August 6, 1992. This work was supported by Scientific Research Grant-in-Aid (03044021) from the Ministry of Education, Science, and Culture of Japan.

The authors are with the Department of Electrical Communications, Faculty of Engineering, Sendai 980, Japan.

IEEE Log Number 9206319.

of medical application of laser light, the small core waveguides with low-losses have been required. In a previous paper [4], we showed numerically based on the exact characteristic equation that the mode transition takes place with decreasing core diameter and the modes in small core waveguides are no more characterized by the well-known modes in large core waveguides.

In this paper, we present an analytical method to predict the relation between hybrid modes in small and large core circular waveguides by using an asymptotic theory. The relation obtained in the singly cladded hollow waveguides is shown to agree with that obtained numerically. The change of the HE_{11} mode in arbitrary singly cladded hollow waveguides is estimated in the plane of the complex refractive index. Finally, mode changes in the dielectric-coated hollow waveguides are also made clear which depend on the thickness of the coated dielectric. Throughout the paper, the wavelength is assumed to be 10.6 μm.

II. Analysis for Singly Cladded Hollow Waveguides

We consider a waveguide consisting of a cylinder of radius T and refractive index $n_0(\simeq 1)$ embedded in a medium with a refractive index $n_0 n_1$. Let the z-components of electric field E_z and magnetic field H_z in the hollow core be expressed in the cylindrical coordinate system (r, θ, z) by

$$E_z = J_n\left(u_0 \frac{r}{T}\right) \cos(n\theta + \theta_0) \tag{1}$$

$$H_z = -\frac{\beta}{\omega\mu_0} P J_n\left(u_0 \frac{r}{T}\right) \sin(n\theta + \theta_0) \tag{2}$$

Then the exact characteristic equations to determine the normalized transverse phase constant in the core $(r < T)u_0$ are given by [4]

$$(\eta_0 - \eta_1)(\eta_0 - n_1^2\eta_1) = n^2\left(\frac{1}{u_0^2} - \frac{1}{u_1^2}\right)\left(\frac{1}{u_0^2} - \frac{n_1^2}{u_1^2}\right) \tag{3}$$

$$u_1^2 - u_0^2 = (n_1^2 - 1)(n_0 k_0 T)^2 \tag{4}$$

where η_0 and η_1 are defined by

$$\eta_0 = \frac{J_n'(u_0)}{u_0 J_n(u_0)} \tag{5}$$

$$\eta_1 = \frac{H_n^{(2)'}(u_1)}{u_1 H_n^{(2)}(u_1)} \tag{6}$$

and u_1 is the normalized transverse phase constant in the cladding $(r > T)$. The parameter P used for the mode designation [4], [5] is expressed by

$$P = n\left(\frac{1}{u_0^2} - \frac{1}{u_1^2}\right) \Big/ (\eta_0 - \eta_1) \tag{7}$$

We now discuss modes in waveguides with arbitrary core radius T. Even if we consider practical small core waveguides, we can assume that $n_0 k_0 T$ is still large compared with unity. By simplifying the characteristic equations by using

$$n_0 k_0 T \gg 1 \tag{8}$$

(3) becomes

$$\left(\eta_0 + j\frac{z_{\mathrm{TE}}}{n_0 k_0 T}\right)\left(\eta_0 + j\frac{y_{\mathrm{TM}}}{n_0 k_0 T}\right) = \frac{n^2}{u_0^4} \tag{9}$$

where z_{TE} and y_{TM} are defined by

$$z_{\mathrm{TE}} = \frac{1}{\sqrt{n_1^2 - 1}} \tag{10}$$

$$y_{\mathrm{TM}} = \frac{n_1^2}{\sqrt{n_1^2 - 1}}. \tag{11}$$

Although y_{TM} is simply related to z_{TE} in the waveguide with a single cladding, we can regard (9) as more general characteristic equation for the waveguide characterized by the normalized surface impedance z_{TE} and admittance y_{TM} at the core-cladding boundary [1].

By solving η_0 from (9), one obtains

$$\eta_0 = \frac{1}{2}\left[-j\frac{1}{n_0 k_0 T}(z_{\mathrm{TE}} + y_{\mathrm{TM}}) + A_{\pm}\right] \tag{12}$$

where $A_{\pm}$ and the parameter P are defined by

$$A_{\pm} = \pm\left[\frac{4n^2}{u_0^4} - \frac{1}{(n_0 k_0 T)^2}(z_{\mathrm{TE}} - y_{\mathrm{TM}})^2\right]^{1/2} \tag{13}$$

$$P = \frac{n}{u_0^2}\frac{1}{\eta_0 + j\dfrac{z_{\mathrm{TE}}}{n_0 k_0 T}} = \frac{n}{u_0^2}\frac{2}{A_{\pm} + j\dfrac{1}{n_0 k_0 T}(z_{\mathrm{TE}} - y_{\mathrm{TM}})}. \tag{14}$$

One should note that $A_{\pm}$ and P explicitly depend on z_{TE} and y_{TM} through $(z_{\mathrm{TE}} - y_{\mathrm{TM}})/n_0 k_0 T$.

We consider the two limiting cases. The first case is

$$|z_{\mathrm{TE}} - y_{\mathrm{TM}}| \ll n_0 k_0 T \quad \text{and} \quad n_0 k_0 T \gg 1 \tag{15}$$

i.e., the case when the core diameter is sufficiently large. From (13), one obtains $A_{\pm}$

$$A_{\pm} = \pm\frac{2n}{u_0^2} \tag{16}$$

and from (12) and (14)

$$P = \begin{cases} 1 & \text{for } A+ \\ -1 & \text{for } A- \end{cases} \tag{17}$$

Equation (17) shows that A_+ and A_- correspond to the EH_{nm} and HE_{nm} modes [5], respectively. The second case is

$$|z_{\mathrm{TE}} - y_{\mathrm{TM}}| \gg n_0 k_0 T \tag{18}$$

which is satisfied for small core waveguides. From (13), one obtains $A_{\pm}$ as

$$A_{\pm} = \pm j\frac{1}{n_0 k_0 T}(z_{\mathrm{TE}} - y_{\mathrm{TM}}) \tag{19}$$

and from (12) and (14)

$$P = \begin{cases} 0 & \text{for } A+ \\ \infty & \text{for } A- \end{cases} \tag{20}$$

It is seen that A_+ and A_- correspond to the TM and TE modes, respectively.

As the mode designation has been made for two limiting cases described by (15) and (18), we next have to make clear how $A_{\pm}$ in the large core waveguide approaches continuously $A_{\pm}$ or $A_{\mp}$ in the small core waveguide. Generally speaking, u_0 changes with the core diameter. However, we assume here that u_0 is equal to $u_0 (= u_\infty + j u_i)$ in the case defined by (15) and furthermore the real part of u_0 does not change. Therefore, u_∞ of the HE_{nm} or EH_{nm} mode is fixed to the zero point of $J_{n-1}(x)$ or $J_{n+1}(x)$ and u_i is equal to

$$u_i = \frac{1}{2}\frac{u_\infty}{n_0 k_0 T}\,\mathrm{Re}(z_{\mathrm{TE}} + y_{\mathrm{TM}}) \tag{21}$$

As u_∞ is much larger than u_i when the core diameter is large, $A_{\pm}$ is expressed by

$$A_{\pm} = \pm\left\{\frac{4n^2}{u_\infty^4}\left[1 - j\frac{2}{n_0 k_0 T}\mathrm{Re}(z_{\mathrm{TE}} + y_{\mathrm{TM}})\right] - \frac{1}{(n_0 k_0 T)^2}(z_{\mathrm{TE}} - y_{\mathrm{TM}})^2\right\}^{1/2} \tag{22}$$

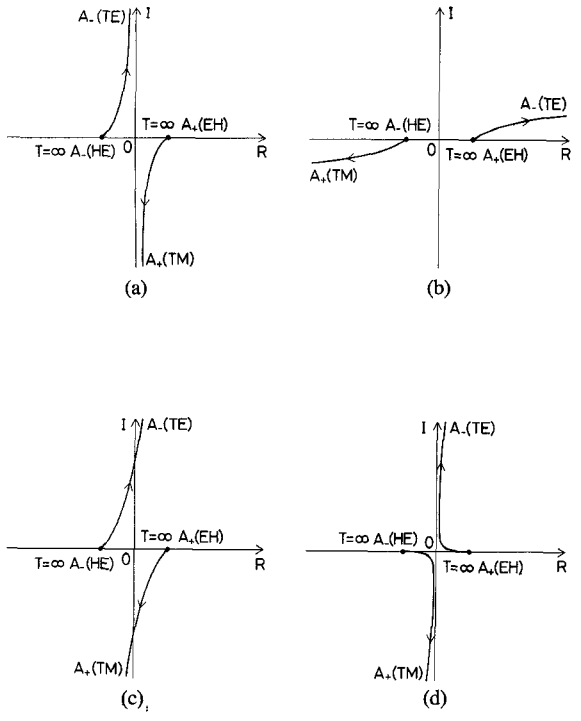

Fig. 1. Schematic loci of $A_{\pm}$ of hybrid modes in various hollow waveguides in the complex plane, where the direction of arrows means decreasing of core diameter. (a) HE_{1m} and $EH_{1m}(m = 1, 2, \cdots, 5)$ modes in a Ge hollow waveguide. (b) HE_{1m} and $EH_{1m}(m = 1, 2, \cdots, 5)$ modes in Ni, Al_2O_3, and SiC hollow waveguides. (c) HE_{11}, HE_{12}, and EH_{11} modes in a SiO_2 hollow waveguide. (d) $HE_{1m}(m = 3, 4, 5)$ and $EH_{1m}(m = 2, 3, \cdots, 5)$ modes in a SiO 2 hollow waveguide.

One should note that (22) is a function of only $n_0 k_0 T$ under fixed material parameters z_{TE} and y_{TM} and mode parameter n.

We now discuss the mode transitions or changes based on (22). As examples, we consider germanium (Ge, $n_1 = 4.0$ [6]), nickel (Ni, $n_1 = 7.39 - j39.3$ [6]), sapphire ($Al_2O_3, n_1 = 0.67 - j0.03$ [7]), silicon carbide (SiC, $n_1 = 0.059 - j1.21$ [6]), and silica ($SiO_2, n_1 = 2.2 - j0.1$ [6]) hollow waveguides.

For the hybrid HE_{1m} and $EH_{1m}(m = 1, 2, \cdots, 5)$ modes in a Ge hollow waveguide, the loci of $A_{\pm}$ of (22) are schematically shown in the complex plane in Fig. 1(a) when the core diameter changes. As the core diameter becomes small, A_+ and A_- in (16) approach A_+ and A_- in (19), respectively. Therefore, the HE_{1m} and EH_{1m} modes change to the TE and TM modes, respectively.

Fig. 1(b) schematically shows loci of $A_{\pm}$ in Ni, Al_2O_3, and SiC hollow waveguides. It is seen that the HE $_{1m}$ and EH_{1m} modes change to the TM and TE modes, respectively, which is different from the result in the Ge waveguide.

We next mention mode transition in a SiO_2 hollow waveguide. The local behaviors of $A_{\pm}$ in the complex plane depend on the mode order. Fig. 1(c) shows the loci of $A_{\pm}$ of the HE_{11}, HE_{12}, and EH_{11} modes, and Fig. 1(d) shows the loci of $A_{\pm}$ of the $HE_{1m}(m = 3, 4, 5)$ and $EH_{1m}(m = 2, 3, \cdots, 5)$ modes. The HE_{11} and HE_{12} modes change to the TE mode and the HE $_{1m}(m = 3, 4, 5)$ modes to the TM mode. Although the method itself is approximate in the sense that $\mathrm{Re}(u_0)$ is fixed, all of the results mentioned above are perfectly coincident to those obtained numerically [4], which suggests that we can predict mode transitions of hybrid modes by using (22) for hollow waveguides consisting of arbitrary claddings. Here, we estimate the region in the plane of the complex refractive index of the cladding material where the

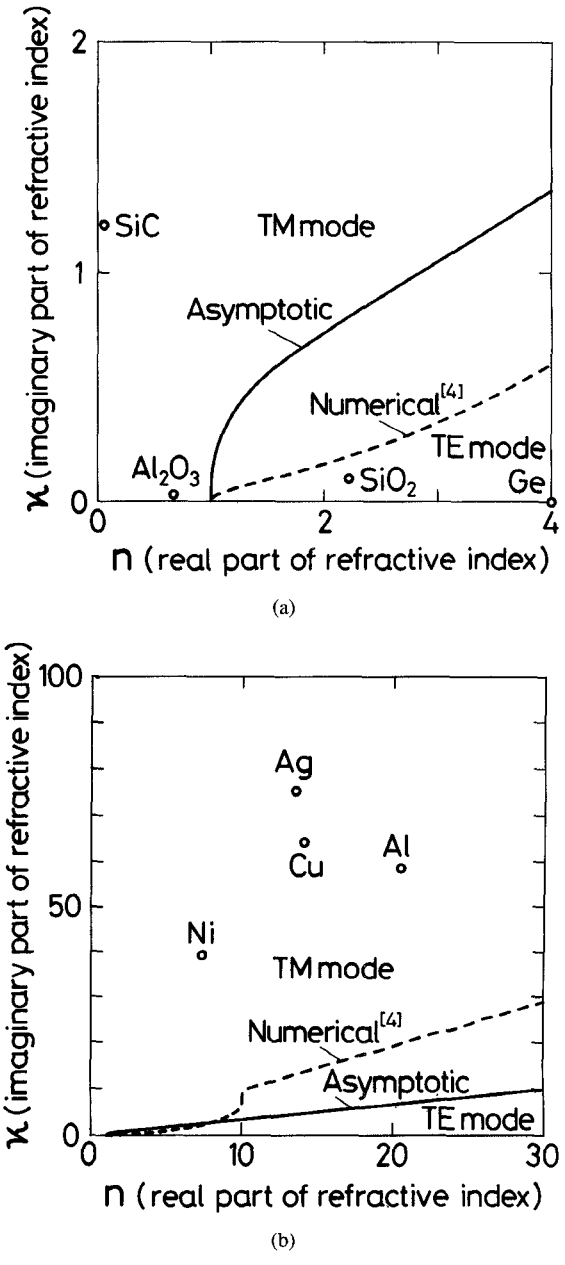

Fig. 2. Boundary curve dividing the TE and TM modes in a small core waveguide corresponding to the HE_{11} mode in the plane of the complex refractive index of the cladding material. The solid and dashed lines correspond to those obtained by the present method and by numerical method [4] for a 0.1 mm core diameter, respectively. The circles correspond to the refractive indices of various cladding materials [6]–[8] at the wavelength of 10.6 μm. (a) $n \leq 4$. (b) $n \leq 30$.

HE_{11} mode in the large core waveguide approaches the TE or TM mode.

Fig. 2(a) and (b) show the boundary curve of this mode change in the plane of the complex refractive index $(n - j\kappa)$ of the cladding material. For comparison, the boundary curve [4] determined based on the exact characteristic equation for a waveguide with a 0.1 mm core diameter is also shown in the figures. Although the method obtaining the boundary curve itself is approximate, the approximation is fairly good for predicting mode designation in practical waveguides. In the region where n is smaller than unity, the HE_{11} mode tends to approach the TM mode. However, when n is larger than unity, the HE_{11} mode tends to approach the TE or TM mode depending on κ.

III. Analysis for Dielectric-Coated Hollow Waveguides

In this section, we investigate mode changes in the dielectric-coated hollow waveguides. For these waveguides, the method mentioned in Sec. II is adopted by using the normalized surface impedance z_{TE} and admittance y_{TM} which are defined by [1]

$$z_{TE} = \frac{1}{\sqrt{a^2-1}} \frac{\sqrt{a^2-1} + j\sqrt{n_1^2-1}\tan(n_0k_0t\sqrt{a^2-1})}{\sqrt{n_1^2-1} + j\sqrt{a^2-1}\tan(n_0k_0t\sqrt{a^2-1})} \tag{23}$$

$$y_{TM} = \frac{a^2}{\sqrt{a^2-1}} \frac{\frac{\sqrt{a^2-1}}{a^2} + j\frac{\sqrt{n_1^2-1}}{n_1^2}\tan(n_0k_0t\sqrt{a^2-1})}{\frac{\sqrt{n_1^2-1}}{n_1^2} + j\frac{\sqrt{a^2-1}}{a^2}\tan(n_0k_0t\sqrt{a^2-1})} \tag{24}$$

where t is a thickness of the coated dielectric which is independent of the core diameter T, a and $n_1$are relative refractive indices of the coated dielectric and cladding, respectively. The attenuation constant α in the waveguides with large core diameter is approximated by [1]

$$\alpha = \frac{1}{2}\frac{n_0k_0u_\infty^2}{(n_0k_0T)^3}\mathrm{Re}(z_{TE} + y_{TM}) \tag{25}$$

By considering that $|n_1| \gg a$, it is seen that there periodically exist optimum thicknesses $(t_1, t_2, t_3, \cdots)$ of the coated dielectric layer where the attenuation becomes minimum. The optimum thicknesses are approximated by [1]

$$t_{2s+1} \simeq \frac{1}{n_0k_0\sqrt{a^2-1}}\left[\tan^{-1}\left(\frac{a}{\sqrt[4]{a^2-1}}\right) + s\pi\right] \quad (s = 0, 1, 2, \cdots) \tag{26}$$

$$t_{2s} \simeq \frac{1}{n_0k_0\sqrt{a^2-1}}\left[-\tan^{-1}\left(\frac{a}{\sqrt[4]{a^2-1}}\right) + s\pi\right] \quad (s = 1, 2, 3, \cdots) \tag{27}$$

We now consider mode transitions in the waveguides with minimum attenuations, i.e., for the cases $t = t_1$ and t_2. Table I summarizes optical constants of the coated dielectric and related parameters of Ge coated silver (Ag, $n_1 = 13.8 - j75.4$ [8]) (Ge/Ag), zinc-sulphide coated Ag (ZnS/Ag), and calcium-fluoride coated Ag (CaF_2/Ag) hollow waveguides. When the thickness t of dielectric layer is t_1 (the thinnest optimum thickness), the loci of the $A_\pm$ of the hybrid HE_{1m} and EH_{1m} modes $(m = 1, 2, \cdots, 5)$ are schematically shown in Fig. 3(a). One can see that the HE_{1m} and EH_{1m} modes change to the TM and TE modes, respectively. On the other hand, when the thickness of the coated dielectric is t_2 (the secondary thinner optimum thickness), the HE_{1m} and EH_{1m} modes change to the TE and TM modes, respectively as schematically shown in Fig. 3(b). It should be noted that the mode properties for t_{2s+1} and $t_{2s+2}(s = 1, 2, \cdots)$ are the same with those for t_1 and t_2, respectively. These mode changes are not affected by the coated dielectrics. Moreover, these are perfectly coincident to those obtained numerically which will be described in a future publication more in detail.

IV. Conclusions

We have investigated mode transitions of the hybrid modes in small and large core circular hollow waveguides by using the asymptotic theory. The mode changes in several singly cladded hollow waveguides are made clear and it is shown that they are coincident to those obtained numerically. The mode changes depend on the cladding material and mode order. The region where the HE_{11} mode changes to the TE or TM mode is shown in the plane of the complex refractive index of the cladding material. The specified region predicted by the approximate theory is fairly coincident to that obtained by using the exact characteristic equation. Moreover, the mode changes of the dielectric-coated hollow waveguides are discussed. The HE_{1m} (EH_{1m}) modes change to the TM (TE) modes, in the case of the thinnest optimum thickness of the coated dielectric, whereas they change to the TE (TM) modes, in the case of the secondary thinner optimum thickness.

TABLE I
Refractive Indices α [6] (Imaginary Parts are Equal to Zero), the Thinnest and Secondary Thinner Optimum Thickness (t_1 and t_2) of the Coated Dielectrics, and Values of $z_{TE} - y_{TM}$ in Various Dielectric -Coated Hollow Waveguides at the Wavelength of 10.6 μm.

Dielectric	a	$t_1(\mu m)$	$z_{TE} - y_{TM}\|_{t_1}$	$t_2(\mu m)$	$z_{TE} - y_{TM}\|_{t_2}$
Ge	4.0	0.46	$-0.0382 + j2.57$	0.86	$-0.0374 - j2.56$
ZnS	2.2	0.84	$-0.0120 + j2.36$	1.82	$-0.0122 - j2.40$
CaF_2	1.28	1.99	$-0.00754 + 4.57j3.17$		$-0.00762 - j3.28$

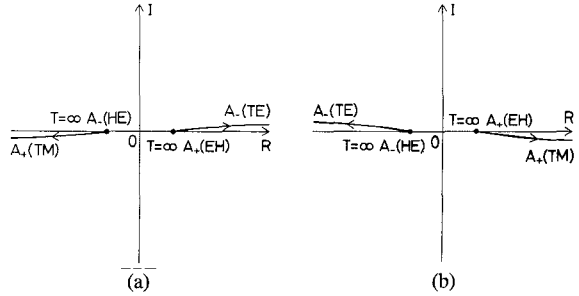

Fig. 3. Schematic loci of $A_\pm$ of HE_{1m} and $EH_{1m}(m = 1, 2, \cdots, 5)$ modes in Ge/Ag, ZnS/Ag, and CaF_2/Ag hollow waveguides in the complex plane. (a) $t = t_1$ (the thinnest optimum thickness). (b) $t = t_2$ (the secondary thinner optimum thickness).

References

[1] M. Miyagi and S. Kawakami, "Design theory of dielectric-coated circular hollow waveguides for infrared transmission," *IEEE J. Lightwave Technol.*, vol. LT-2, pp. 116–126, May 1984.

[2] A. Hongo, K. Morosawa, T. Siota, K, Suzuki, S. Iwasaki, and M. Miyagi, "Transmission of 1 kW-class CO_2 laser light through circular hollow waveguides for material processing," *Appl. Phys. Lett.*, vol. 58, no. 15, pp. 1582–1584, Apr. 1991.

[3] S. J. Saggese, J. A. Harrington, and G. H. Sigel, Jun., "Hollow sapphire waveguides for remote radiometric temperature measurements," *Electron. Lett.*, vol. 27, no. 9, pp. 707–709, Apr. 1991.

[4] Y. Kato and M. Miyagi, "Modes and attenuation constants in circular hollow waveguides with small core diameters for the infrared," *IEEE Trans. Microwave Theory Tech*, vol. 40, pp. 679–685, Apr. 1992.

[5] E. Snitzer, "Cylindrical dielectric waveguide modes," *J Opt. Soc. Am.*, vol. 51, no. 5, pp. 491–498, May 1961.

[6] E. D. Palik, Ed., *Handbook of Optical Constants of Solids*, Orlando, FL: Academic Press, 1985, pp. 280–764, Pt. 2.

[7] J. A. Harrington and G. C. Gregory, "Hollow sapphire fibers for the delivery of CO_2 laser energy," *Opt Lett.*, vol. 15, no. 10, pp. 541–543, May 1990.

[8] K. Kudo, *Kiso Bussei Zuhyo* (Table of Fundamental Properties of Materials), Kyoritsu Shuppan, Tokyo, Japan: 1972, pp. 128–133 (in Japanese).